the FEBS Journal

An asymmetric ion channel derived from gramicidin A

Synthesis, function and NMR structure

Xiulan Xie[1], Lo'ay Al-Momani[1], Philipp Reiß[1], Christian Griesinger[2] and Ulrich Koert[1]

1 Fachbereich Chemie, Philipps-Universität Marburg, Germany
2 Max-Planck Institut für Biophysikalische Chemie, Göttingen, Germany

Keywords
asymmetric D, L-peptides; CD spectroscopy; DYANA NMR structure; ion channel; β-helix

Correspondence
U. Koert, Fachbereich Chemie, Philipps-Universität Marburg, Hans-Meerwein-Strasse, 35032 Marburg, Germany
Fax: +49 6421 282 5677
Tel: +49 6421 282 6970
E-mail: koert@chemie.uni-marburg.de

(Received 1 October 2004, revised 16 November 2004, accepted 16 December 2004)

doi:10.1111/j.1742-4658.2004.04531.x

The biological ion channel gramicidin A (gA) was modified by synthetic means to obtain the tail-to-tail linked asymmetric gA-derived dimer compound **3**. Single-channel current measurements for **3** in planar lipid bilayers exhibit an Eisenman I ion selectivity for alkali cations. The structural asymmetry does not lead to an observable functional asymmetry. The structure of **3** in solution without and with Cs cations was investigated by ^{1}H-NMR spectroscopy. In $CDCl_3/CD_3OH$ (1 : 1, v/v), **3** forms a mixture of double-stranded β-helices. Upon addition of excess CsCl, the double-stranded species are converted completely into one new conformer: the right-handed single-stranded β-helix. A combination of DQF-COSY and TOCSY was used for the assignment of the ^{1}H-NMR spectrum of the Cs–**3** complex in $CDCl_3/CD_3OH$ (1 : 1, v/v). A total of 69 backbone, 27 long-range, and 64 side-chain distance restraints were obtained from NOESY together with 25 ϕ and 14 χ_1 torsion angles obtained from coupling constants. These data were used as input for structure calculation with DYANA built in SYBYL 6.8. A final set of 11 structures with an average rmsd for the backbone of 0.45 Å was obtained (PDB: 1TKQ). The structure of the Cs–**3** complex in solution is equivalent to the bioactive channel conformation in the membrane environment.

Ion channels are biomolecular key functions, which allow the passive transport of ions through a phospholipid bilayer [1]. A concentration gradient or an electrical potential can be the driving force for the channel transport. Much progress has been made in the structural understanding of biological ion channels mainly by means of X-ray crystallography [2–4]. In line with these efforts stands the goal to engineer biomolecular channels by synthetic means or to design synthetic ion channels [5–7]. Two different approaches towards synthetic ion channels have been investigated so far: a peptide one [8] and a nonpeptide one [9–11] using, for example, ether motifs. In addition, hybrid channels, which combine peptides with synthetic building blocks, are known [12–15].

Gramicidin A (gA) serves as a structural lead for engineering biological ion channels [16–18]. This lipophilic pentadecapeptide with alternating D- and L-configured residues is synthesized by the bacterium *Bacillus brevis* in its sporulation phase. In a phospholipid bilayer, gA functions as a cation channel for alkali cations with a weak Eisenman I selectivity ($Cs^+ > K^+ > Na^+ > Li^+$) [1]. The channel-active conformation of gA in a membrane-like environment was postulated by Urry [19] to be a head-to-head dimer of two single-stranded β-helices. This structure was confirmed in micelles using liquid-state NMR [20,21] and in a phospholipid bilayer by solid-state NMR [22]. In organic solvents, gA forms a multitude of generally dimeric β-helical species [23,24]. Based on the solid-state NMR structure, the energetics of ion conduction through the gramicidin channel have been calculated [25]. Solid-state structures of gA with different cations have been obtained by X-ray

Abbreviations
DMPC, dimyristoylphosphatidylcholine; gA, gramicidin A.

crystallography and discussed in the context of the channel-active conformation [26–28].

Covalent linkage of the two N-termini of the gA strands in the head-to-head dimer confines the conformational space, leading to unimolecular channels which facilitates structural studies. A suitable substitute for two formamides is a C_4-linker [29]. During our studies of tetrahydrofuran–gA hybrids [12,30] and cyclohexylether–gA hybrids [13], a related succinate linker was used. Upon reduction of the pentadecapeptide sequence of gA to 11 residues, the minigramicidin **1** results. Minigramicidin (**1**) as well as its covalent dimer (**2**) have been synthesized, and their hydrophobic match with the membrane studied [31]. The structures of **2** in organic solvents with and without cations have been thoroughly studied by NMR [32]. In the absence of metal ions, the structure of **2** in the two solvent mixtures [$^2H_6$]benzene/[$^2H_6$]acetone (10 : 1, v/v) and $CDCl_3$/CD_3OH (1 : 1, v/v) has been determined to be a left-handed double β-helix with 5.7 residues per turn. Upon addition of excess of the metal ion Cs^+, a structural change took place. The left-handed double-helix structure transformed into two single-stranded right-handed β-helices with 6.3 residues per turn. Whereas the left-handed double β-helix is consistent with the structure of gA obtained in the presence of $CaCl_2$ in methanol [33], the single-stranded right-handed β-helix agrees with the ion-channel-active structure of gA in the membrane [22]. It was thus concluded that for **2**, the binding of Cs^+ to the linked gA switches the double-helix structure into its ion-channel-active conformation [32] (Fig. 1).

Biological ion channels are asymmetric structures. In the case of the KcsA channel, the selectivity filter is positioned at the outside of the cell membrane and the gate is located at the cytoplasmic side [2]. This structural asymmetry is connected with the biological function of the KcsA channel: the transport of cations from the exterior to the interior. A covalent linkage of a shorter gA sequence with a longer gA sequence would generate an asymmetric channel structure.

Compound **2** is a covalently linked symmetric channel. To study asymmetric channels of the gramicidin type, we focused on asymmetric covalently linked gA-type dimers. Here, we report on the synthesis, functional analysis (single-channel current measurements) and structural studies (NMR, CD) of a novel asymmetric linked dimer **3**. Points of interest are, first, whether the structural asymmetry in **3** leads to functional asymmetry (two observable channel types resulting from two possible orientations in the membrane) and, second, whether Cs^+-induced

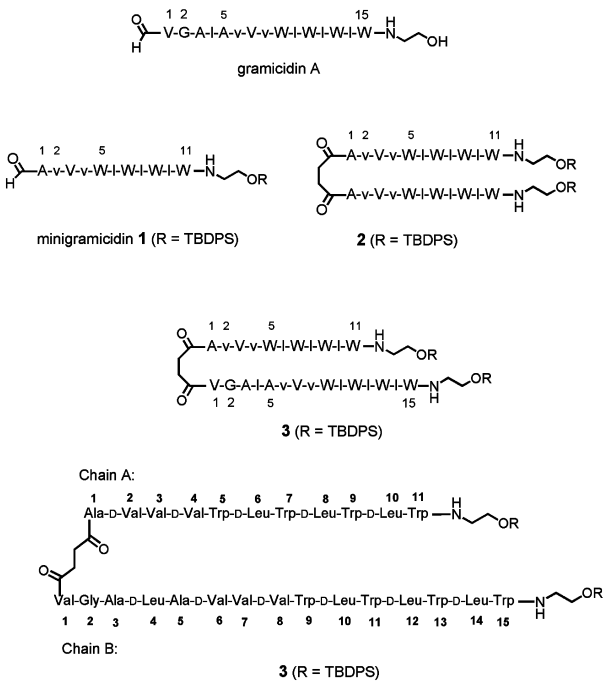

Fig. 1. Structures of gramicidin A, minigramicidin (**1**), linked minigramicidin (**2**) and the linked asymmetric dimer (**3**).

formation of the single-stranded right-handed β-helix takes place in the case of **3**. Compound **3** represents the first structure with an asymmetric structural motif in a linked gA derivative. Mini-gA (11 amino-acid residues, denoted as chain A) and gA (15 residues, denoted as chain B) are linked head-to-head by succinic acid.

Results

Synthesis

Synthesis of the asymmetric linked dimer **3** made use of the segment coupling strategy developed for the synthesis of **2** [34]. Dimer **3** was assembled from the three building blocks **4**, **5** and **6** (Scheme 1). Thus HOBT/HBTU coupling of the succinate–dipeptide **4** with the 11-mer **5** produced compound **7**. After hydrogenolytic cleavage of the benzyl ester in **7,** a HOAT/HATU coupling with the 13-mer, **6**, gave the desired target compound **3**.

The product, **3**, was purified by chromatography (10 g silica gel, chloroform/methanol/formic acid [100 : 3 : 7 (v/v/v) to 100 : 4 : 7 (v/v/v); neutralization of formic acid followed the flash column chromatography to give **3** as a colourless solid. Analytical and preparative HPLC: Caltrex; A, H_3PO_4/NaH_2PO_4 buffer, pH 3; B, methanol, 90% → 100% B. ^{1}H-NMR (500 MHz,

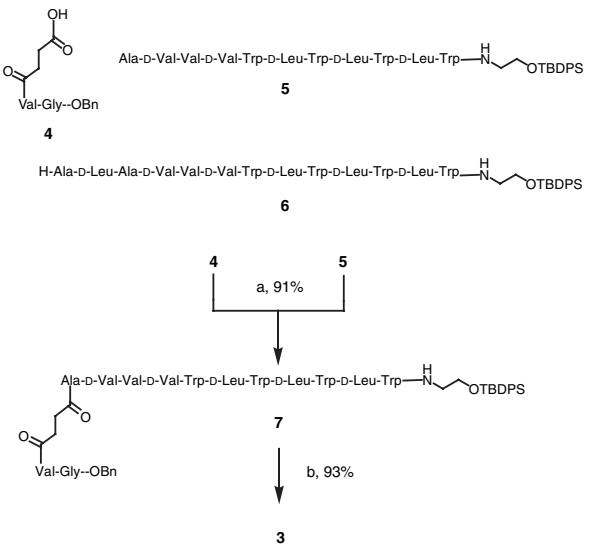

Scheme 1. (a) HOBt/HBTU, DIEA, dichloroethylene/dimethylformamide, −10 °C, 91%; (b) debenzylation of **7**: H_2, Pd/C, methanol; coupling: HOAt/HATU, diisopropylethylamine, DMF, 0 °C, 90%.

DMSO-d_6, 300 K); see Supplementary material. High resolution MS (ESI): $C_{216}H_{290}N_{36}LiNaO_{30}Si_2$ [M + Na^+ + Li^+] Calc.: 1985.0717, Found: 1985.1092.

Ion channel activity

Single-channel current measurements in planar lipid bilayers were performed in asolectine to characterize the ion-channel activity of **3** [1,12]. Compound **3** displayed the single-channel characteristics of univalent cations (Fig. 2A–D). The asymmetric compound **3** may possess two different configurations in the membrane leading *a priori* to two different types of channel. This possible functional asymmetry is a consequence of its structural asymmetry. Surprisingly, only one type of channel was observed for each cation, which shows that in our case the structural asymmetry of **3** does not lead to functional asymmetry. The succinate linker interrupts the helical arrangement of amide-binding sites for the cation. The position of the succinate linker in the channel seems to have no effect on the ion transport. The following states of conductance of **3** were calculated from the I–V curves (Fig. 2E): Cs^+, 26.6 pS; K^+, 14.2 pS; Na^+, 7.1 pS. The observed selectivity followed an Eisenman I order ($Cs^+ > K^+ > Na^+$) [1]. The channel dwell times were of the order of several seconds.

CD spectra

CD spectra were measured in organic solvents of different polarity, as well as in dimyristoylphosphatidylcholine (DMPC) vesicles. Trifluoroethanol is well known as a disaggregate solvent for proteins and polypeptides. The CD spectrum of **1** in trifluoroethanol with a maximum positive ellipticity around 222 nm (Fig. 3A) indicates a random-coil structure. In methanol, two positive maxima were observed at ≈209 and 230 nm (Fig. 3A). These two maxima are characteristic of a parallel right-handed double helix of gA [24].

A CD spectrum of **3** was measured in a mixture of two organic solvents (dichloroethane/methanol, 1 : 1, v/v), which is equivalent to the NMR measurements in $CDCl_3/CD_3OH$ (1 : 1, v/v). Two positive ellipticity maxima were observed at ≈209 and 230 nm (Fig. 3B), which indicated a parallel right-handed double helix. A dramatic change in the CD spectrum was seen in the presence of 8 eq CsCl. Just one positive maximum

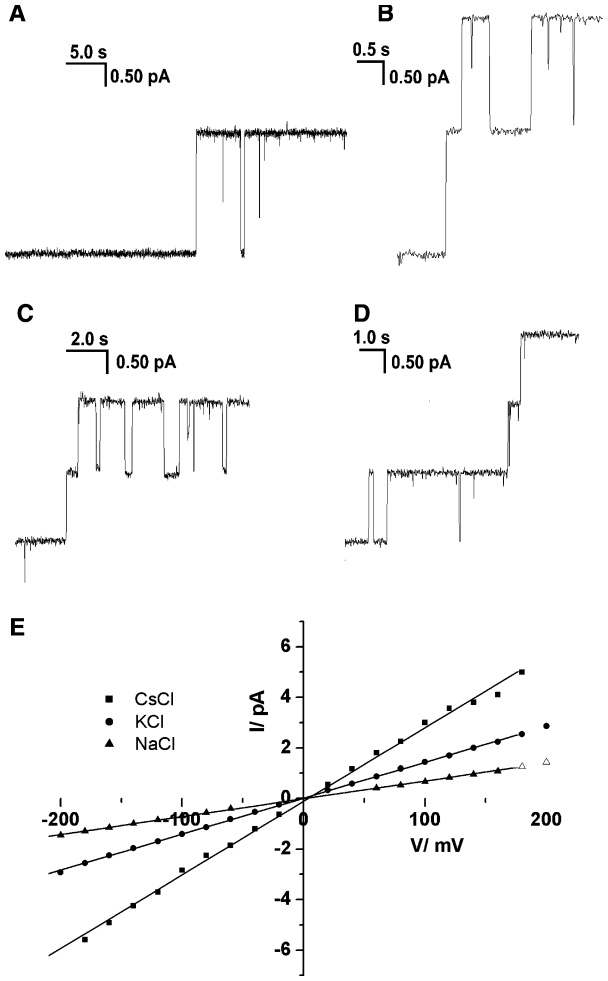

Fig. 2. Current traces of **3** in asolectine at 100 mV. (A) 1 M CsCl; (B) 1 M NH_4Cl; (C) 1 M KCl; (D) 1 M NaCl; (E) current-voltage curves (*I–V* curves) of **3** in asolectine and 1 M solution of CsCl, KCl and NaCl.

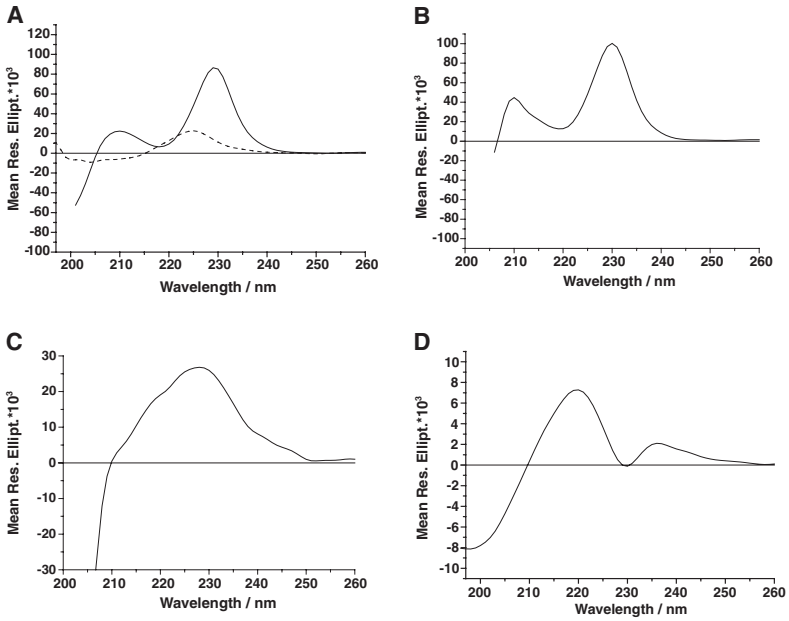

Fig. 3. CD spectra of **3**. (A) In trifluoroethanol (dashed) and methanol (solid); (B) in dichloroethylene/methanol (1 : 1, v/v); (C) in dichloroethylene/methanol (1 : 1, v/v) with 8 eq CsCl; (D) in DMPC vesicles.

with low intensity was observed at ≈228 nm (Fig. 3C). This type of CD spectrum is the same as for the Cs complex of **2** [32]. A CD spectrum of **3** in DMPC vesicles was identical with those of gA and **2** [24,32]. Two maxima were detected at ≈336 nm with low intensity and at ≈219 nm (Fig. 3D).

The CD data point to a double-stranded structure in organic solvents, which changes into a single-stranded structure in the presence of Cs^+ or in a lipid environment.

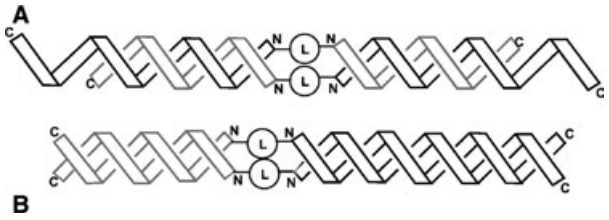

Fig. 4. Two possible double-stranded structures of **3**: (A) antiparallel; (B) parallel.

NMR studies

Unlike the succinyl-linked mini-gA **2**, which has no difference in its parallel and antiparallel secondary structures and forms a single species of double β-helix in organic solution, compound **3** may form more than one double-stranded aggregate. The two major species of the possible conformation are depicted in Fig. 4. Conformations of type **A** (parallel double-helix) and type **B** (antiparallel double-helix) may coexist in solution.

To confirm this assumption, a DQF-COSY spectrum was recorded for **3** in $CDCl_3/CD_3OH$ (1 : 1, v/v; for the spectrum see Fig. S1). In the fingerprint region of the DQF-COSY spectrum (Fig. S1), at least two major conformers could be recognized. By using DQF-COSY, TOCSY, and NOESY, Bystrov & Arseniev [23] showed diversity in the conformation of gA in ethanol. We thus draw a preliminary conclusion that **3** forms at least two conformers in $CDCl_3/CD_3OH$ (1 : 1, v/v). Because of serious overlapping of the NMR resonance signals, NMR structural determination is still under investigation.

As revealed in our previous study with **2** [32], the binding of the Cs^+ ion can trigger the transformation of a double-helix structure into a single-stranded β-helix structure, which corresponds to the ion-channel-active conformation. If this folding process were adaptable to **3**, the multiconformers of **3** in solution should all unwind into a single-stranded β-helix. Therefore, saturation with Cs^+ ion should provide a chance to observe a dominant ion-channel-active conformation of **3** in solution. Titration of **3** in $CDCl_3/CD_3OH$ (1 : 1, v/v) with CsCl was performed, and the process was monitored by recording ^{1}H-NMR spectra. After saturation with CsCl (at concentrations above 10.9 mM), clearly resolved signals in the NH and αH regions of the ^{1}H-NMR spectra were observed (Fig. S2). We thus conclude that, transformation of the multiconformers took place during the titration, and the **3**–Cs^+ complex shows a single dominant

conformer in solution. Owing to serious signal overlapping in the ^{1}H-NMR spectra, especially those of the early titration steps, an unambiguous determination of signal intensity is not possible. Therefore, a titration curve cannot be obtained. In the following, we focus on determination of the structure of the **3**–Cs^+ complex.

Mixtures of apolar/polar solvents ($CDCl_3/CD_3OH$ and C_6D_6/CD_3COCD_3) were used to mimic the dielectric constant of membrane environments [35]. Fine-tuning of the ratio of the solvents is necessary for each specific polypeptide to obtain a pure dominant secondary structure [32]. NMR spectra (NH and αH region of ^{1}H and fingerprint region of DQF-COSY) were recorded for samples in different solvent mixtures at different ratios. It was found that the **3**–Cs^+ complex adopts a pure dominant structure in $CDCl_3/CD_3OH$ (1 : 1, v/v) or C_6D_6/CD_3COCD_3 (10 : 1, v/v). In the following, the results for the **3**–Cs^+ complex in $CDCl_3/CD_3OH$ (1 : 1, v/v) are presented.

For structure determination, NMR spectra of DQF-COSY, TOCSY, and NOESY with mixing times of 150 ms and 300 ms were recorded. Assignments were obtained by standard procedures [36]. A combination of DQF-COSY and NOESY produced sequential assignments (i.e. all αH and NH and their sequence in the backbone), and a combination of DQF-COSY and TOCSY resulted in assignments of the side chains. The molecule has a special structural motif: asymmetric with similarity in chains A and B (chain B = Val-Gly-Ala-D-Leu-chainA; Fig. 1). As a result, all the amino-acid residues are in different chemical environments and therefore show different chemical shifts. However, owing to the similarity in chains A and B, the difference in chemical shifts between the residues in A and those of the corresponding sequence in B is very small. Even when recorded on an 800-MHz spectrometer, the signals were not fully resolved. Unambiguous assignments of side chains were only possible up to the β-position and γ-position of valines. For detailed assignments see Table S1.

Figure 5 shows the fingerprint region of a DQF-COSY spectrum with full assignments. COSY cross-peaks in this region show coherence between intraresidue NH and αH.

Two pieces of information can be obtained from this spectrum: (a) the number of cross-peaks reflects the corresponding number of residues in the polypeptide; (b) from the trace of the antiphase cross-peak, the coupling constant $^3J_{NH\text{-}\alpha H}$ can be measured ($^3J_{NH\text{-}\alpha H}$

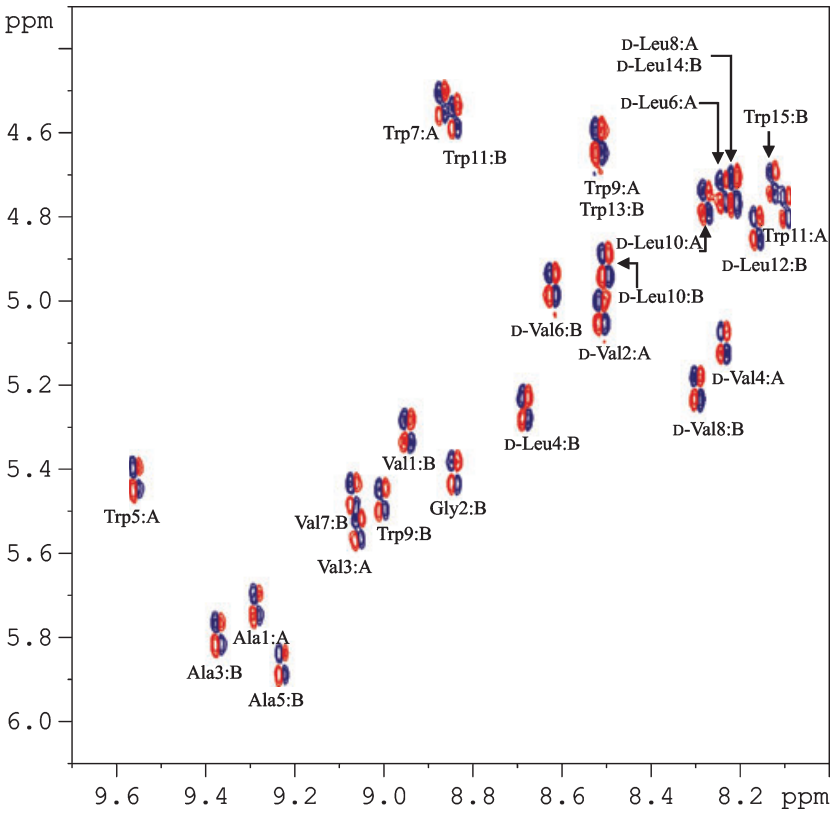

Fig. 5. DQF-COSY spectrum in the region of (F_2) 9.7–8.0 p.p.m. and (F_1) 6.1–4.3 p.p.m. (NH-αH fingerprint region) of **3**–Cs^+ complex in $CDCl_3/CD_3OH$ (1 : 1, v/v) at 293 K.

reflects the type of secondary structure and can also be used to calculate the torsion angle ϕ; see the section Structure determination). As shown in Fig. 5, the cross-peaks of Trp9:A and Trp13:B, as well as the cross-peaks of D-Leu8:A and D-Leu14:B overlap into one peak. The rest of the cross-peaks are all well resolved. The clarity and complete assignment of the cross-peaks confirm a pure conformer of the complex. The $^{3}J_{\mathrm{NH}\text{-}\alpha\mathrm{H}}$ coupling constants measured are in the range 8.8–9.9 Hz (Table S2), which is typical of a β-sheet.

Figure 6 shows the fingerprint region of a 150-ms NOESY spectrum with full sequential assignments. In this region, three types of peak were observed: sequential cross-peaks between $\alpha\mathrm{H}_i$ and NH_{i+1} (the index shown in subscript stands for a residue's sequence number throughout the manuscript) in blue, intraresidue cross-peaks between $\alpha\mathrm{H}_i$ and NH_i in yellow, and long-range inter-residue NOEs in red. The long-range NOEs observed can be ascribed to two types: those between $\alpha\mathrm{H}_i$ and NH_{i+6} ($i = 1$, 3, and 5 for chain A, and 1, 3, 5, 7, and 9 for chain B); and those between $\alpha\mathrm{H}_i$ and $\mathrm{NH}_{i\text{-}6}$ ($i = 10$ and 8 for chain A, and 14, 12, 10, and 8 for chain B). These two types of long-range NOE reflect a right-handed single-stranded β-helix with about six residues per turn (for a schematic view see Fig. S3). This proposed structure agrees well with the ion-channel-active conformer of gA in the membrane [22] and the Cs^+ complex of **2** in solution [32].

As the CD and NMR (titration, COSY, and NOESY) results hint strongly that the secondary structure of the **3**–Cs^+ complex in $CDCl_3/CD_3OH$ (1 : 1, v/v) is a right-handed single-stranded β-helix, we should be able to observe the hydrogen bonds formed in the secondary structure. This can be realized by recording the temperature dependence of NH chemical shifts [33]. ^{1}H-NMR spectra were thus acquired over the temperature range 278–313 K in 5 K increments. Chemical shifts of the NH of all the residues were extracted and plotted against temperature. Linear dependence was observed, and the dependence was further fitted using ORIGIN 6.0 (Microcal Software Inc, Northampton, MA, USA). The temperature coefficients obtained from the fitted data are shown in Fig. 7.

Owing to the serious signal overlapping, the determined temperature coefficients for the two terminal residues Trp11 of chain A and Trp15 of chain B are highly uncertain (with three and four unambiguous data points and R of 0.98 and 0.98, respectively).

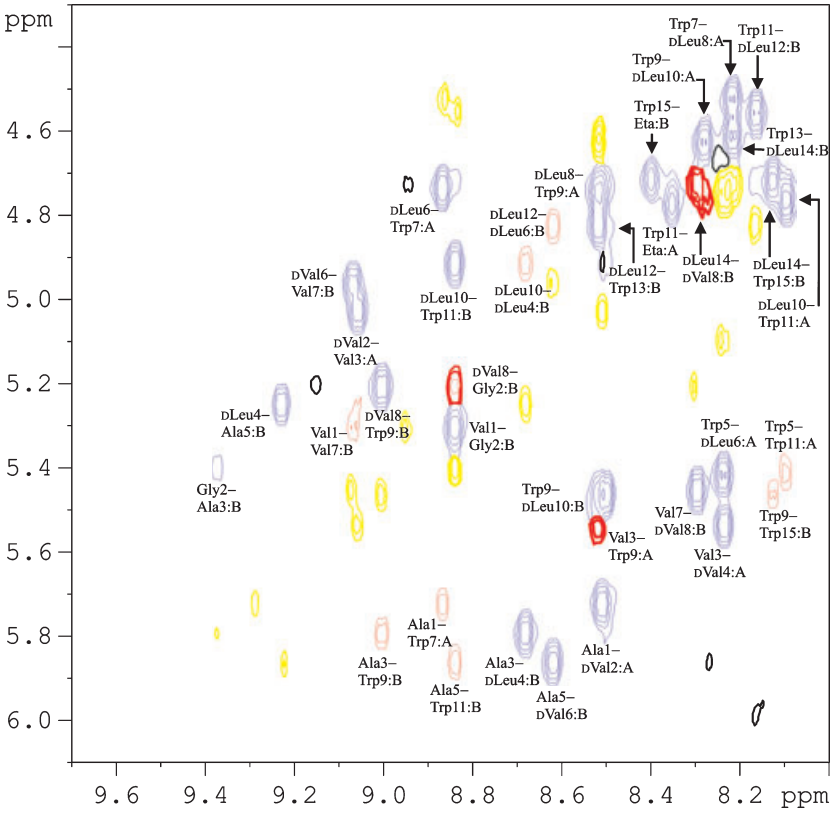

Fig. 6. NOESY spectrum (150 ms) in the region of (F_2) 9.7–8.0 p.p.m. and (F_1) 6.1–4.3 p.p.m. (NH-αH fingerprint region) of **3**–Cs^+ complex in $CDCl_3/CD_3OH$ (1 : 1, v/v) at 293 K.

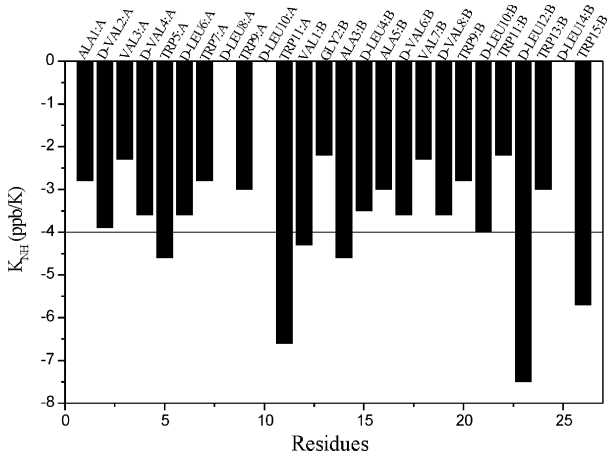

Fig. 7. Plots of NH chemical-shift temperature coefficient against amino-acid residue.

Besides, coefficients for D-Leu8 and D-Leu10 of chain A and D-Leu14 of chain B could not be determined because of strong temperature dependence and the crowdedness of the resonance signals. The coefficient of D-Leu12:B was determined to be -7.5 p.p.b.$\cdot K^{-1}$. Residues D-Leu8:A, D-Leu10:A, D-Leu12:B, and D-Leu14:B are on the terminal turns of the helix; their NHs point outwards from the helix and thus cannot form hydrogen bonds. The remaining residues show temperature coefficients reasonable for hydrogen bond formation.

Structure determination

Structure calculations were performed with DYANA built in SYBYL. Compound **3** contains the nonstandard amino acids D-valine and D-leucine. Molecules of these two residues were thus created and added to the protein dictionary of SYBYL and the standard library of DYANA. In the **3**–Cs^+ complex, chains A and B are connected head-to-head by succinic acid, in such a way that the molecule entity starts from a C-terminus and ends at another C-terminus. Such a nonstandard polypeptide cannot be recognized by the program SYBYL as it is. Pseudo-residues (according to definition in DYANA, PL: combining protein with dummy linker, LL: dummy linker, and LP: combining dummy linker with protein) were applied to solve this problem [37,38]. In the initial structures of random coil, the succinic acid was separated into two groups of acetic acid (named ACU in the PDB structure with an accession code 1TKQ). Five pseudo-residues were used to link chains A and B (ACU-chain:A-PL-LL-LL-LL-LP-ACU-chain:B). In this way, the structure starts from an N-terminus and ends at a C-terminus, which is similar to a normal polypeptide. The chemical bond within the succinic acid was realized by putting a distance constraint $r_{C\text{-}C} = 1.55$ Å between the two ACU groups, in addition to those extracted from NOEs.

As described in the Synthesis section, both of the C-termini of **3** attached with ethanolamine have a capping group *t*-butyldiphenylsilyl, which was applied to enhance the solubility and stability of the structure in organic solvents. Owing to ambiguity in resonance assignment of the termini and therefore a lack of enough NOE constraints, the *t*-butyldiphenylsilyl termini were omitted in the structure calculation.

By using the program module TRIAD in SYBYL, NOE cross-peaks of 150 ms NOESY spectrum were converted into distance constraints. In this way, the following distance constraints were obtained: 69 for backbone, 27 for long-range backbone, and 64 for the side chains. Thus there were on average 6.2 distance constraints per residue.

Based on the measured *J* coupling constants and the Karplus relations [39], orientational constraints can be obtained. Thus, torsion angles ϕ were calculated from $^3J_{NH\text{-}\alpha H}$. Two sets of 25 ϕ were obtain: ϕ_1 ($-140° \approx -130°$) and ϕ_2 ($-110° \approx -100°$) (Table S2). ϕ_1 and ϕ_2 correspond to antiparallel β-sheet and parallel β-sheet, respectively. According to the orientational constraints of gA in membrane [22], torsion angles ϕ_1 were used in our calculation. Based on $^3J_{\alpha H\beta H}$, 14 χ_1 angles were calculated for the residues valine and leucine.

With distance constraints of the backbone and the 25 torsion angles ϕ, preliminary structures were first calculated. Hydrogen bonds in the preliminary structures were identified with distance and angle criteria (donor–acceptor distance shorter than 2.4 Å, hydrogen–donor–acceptor angle smaller than 35°). The 20 hydrogen bonds thus identified are in agreement with the NH temperature coefficients. The hydrogen-bonding pattern between helical turns defined here agrees with that of gA in membrane obtained from solid-state NMR [22].

A final set of constraints containing all the unambiguous NOE distance constraints, hydrogen bond restraints, and torsion angles ϕ and χ_1 was used in the simulated annealing protocol for DYANA calculation. The calculation was initiated with 50 random conformers and resulted in 11 conformers with target function within 0.3 $Å^2$. The 11 conformers were energy-minimized under NMR constraints using the TRIPOS force field implemented in SYBYL 6.8 (Tripos Inc., St Louis, MO, USA). These 11 energy-minimized conformers show an average rmsd for the backbone of 0.45 Å and are kept to represent the solution structure of complex **3**. Figure 8 shows the stereo views of the superimposed backbones of these.

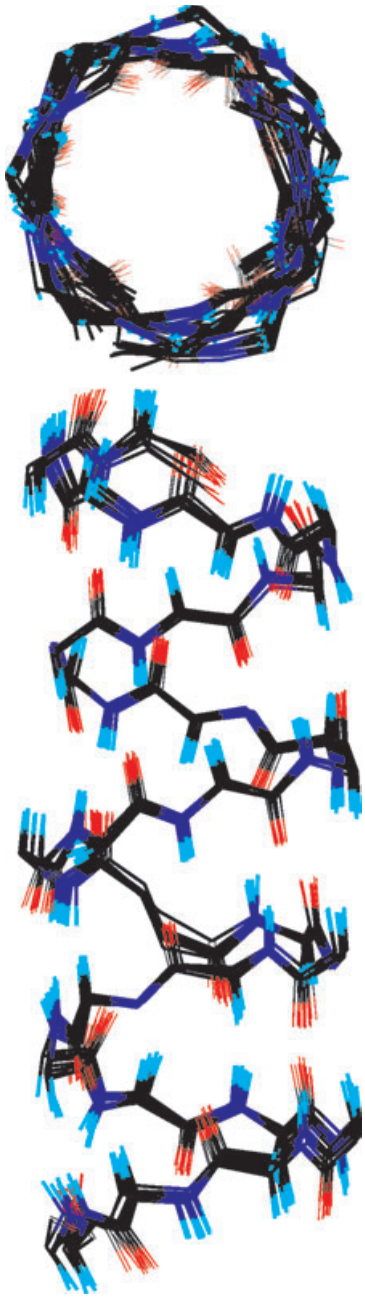

Fig. 8. Stereo view of the superimposed backbones of the 11 lowest target function structures.

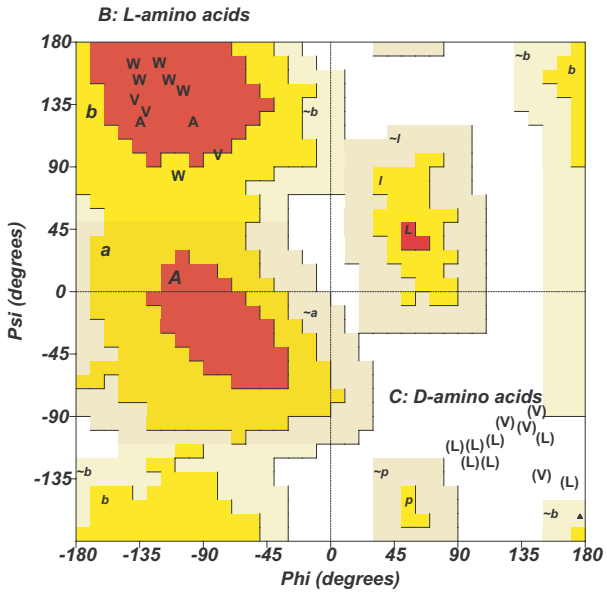

Fig. 9. Ramachandran plot of the averaged structure obtained from the 11 lowest target function structures. All the L-amino acids are within the allowed region of β-helix, and all the D-amino acids are in a region that is a mirror image to β-helix.

The quality of these structures was evaluated using the program PROCHECK [40]. A Ramachandran plot thus generated is shown in Fig. 9. The 11 data points located on the bottom right of the Ramachandran plot arise from the 11 D-amino-acid residues. Nine residues were found to be in the most favorable regions, with two in additional allowed regions. If the D-amino-acid residues, which comprise 50% of the nonterminus residues in the complex, are considered to be in favorable regions, then the apparent percentage of residues in favorable regions calculated will be greatly improved.

As the assignment of side chains was not complete, no stereo assignment was given to leucines and tryptophans. Therefore, the orientations of the indoles are not defined in the structures. The structure has been deposited in the RCSB Protein Data Bank (accession code 1TKQ).

Discussion

Compound **3** forms more than one double-stranded β-helical structure in organic solvents. In the case of the symmetric dimer **2**, one distinct left-handed double-stranded β-helix could be deduced from the NMR data [32]. The structural asymmetry of **3** leads to a structurally more complex picture. No distinct structure could be elucidated from the NMR data of **3** in organic solvents. An inspection of the CD data indicates the presence of double-stranded helices. It is reasonable to assume a mixture of the antiparallel and parallel double helix shown in Fig. 4.

The structurally complex picture simplifies on addition of CsCl. The Cs–**3** complex has the structure of a right-handed single-stranded β-helix (PDB: 1TKQ; Fig. 10A). This was confirmed by solving the NMR structure of **3** with Cs^+ in $CDCl_3/CD_3OH$ (1 : 1, v/v).

The fact that the addition of Cs^+ favors the single-stranded helix was observed with **2** and **3**. This indicates a general trend for head-to-head linked gA dimers: Cs^+ shifts the conformational equilibrium towards the single-stranded helix. The single-stranded structures of the Cs complexes of **2** and **3** are equivalent to the channel-bioactive conformation in the membrane. This stresses the importance of cations in the structures of alternating D,L-peptides. X-ray and NMR studies have so far revealed only double-stranded helices for cation–gA complexes in the solid state and in organic solvents [24]. The examples of the Cs complexes of **2** and **3** demonstrate that, under particular conditions, the single-stranded helix can be dominant in solution too. The covalent linkage performed by the succinate plays a crucial role. A schematic view of the conformational change in **3** on addition of Cs cations is shown in Fig. 10B. The mixture of double-stranded helices **IA** and **IB** dissociates into single-stranded monomers **II**, which bind one and then two Cs^+ cations (→ **III** → IV). Owing to problems with the inexactly defined mixture of the double-stranded conformers, we were not able to determine the stability constants for the Cs complex formation. ESI-MS reveals the major presence of two Cs cations in the complex. No 1 : 1 or 4 : 1 Cs complex of **3** was detected by ESI-MS, but a minor amount of the 3 : 1 complex was present in the gas phase besides the major 2 : 1 complex. The stoichiometry of the Cs complex in solution cannot be defined unambiguously on the basis of the present data. However, the possibility of generating and studying the bioactive conformation of an ion channel in solution should contribute to our understanding of the ion binding and dynamics in the channel pore. The results from such studies should help to clarify the transport mechanism of biological ion channels.

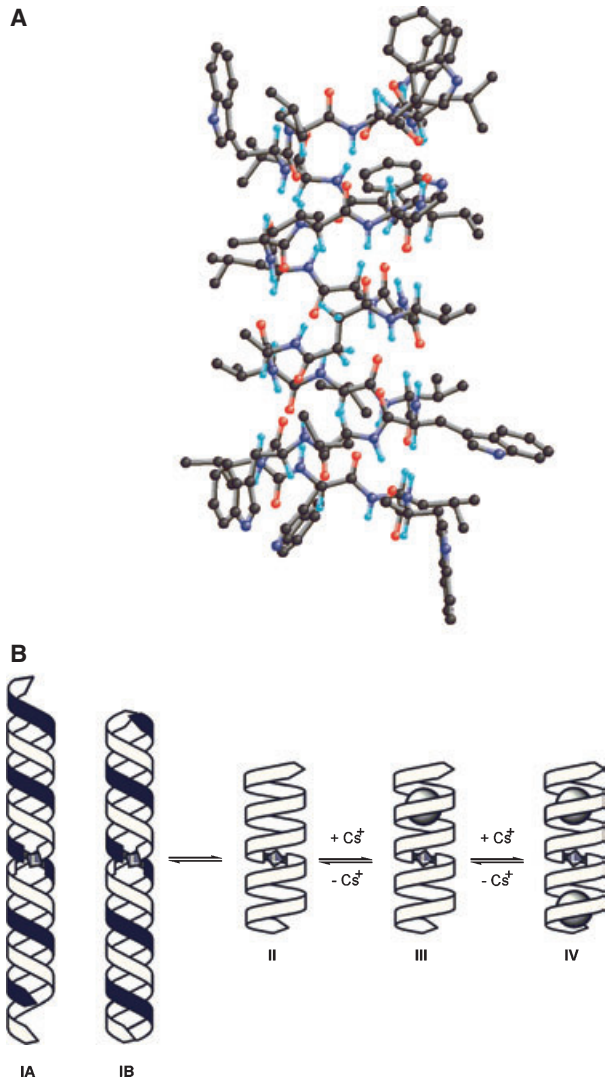

Fig. 10. (A) Stereo view of the average structure obtained from the 11 lowest target function structures for the peptide part of the Cs^+–**3** complex. Side chains are also included. (B) Schematic view of the Cs^+-induced conversion of the mixture of double-stranded helices into the right-handed single-stranded helix.

In conclusion, these results show that the Cs cation effect on the favored formation of the single-stranded β-helix seems to be general for covalently linked gA derivatives. In asymmetric structures such as **3**, the position of the succinate linker has no measurable influence on the overall ion transport through the channel.

Experimental procedures

Synthesis

Chemicals and reagents were purchased from Aldrich, Sigma, Fluka, Bachem and used without further purification. Solvents were purified by distillation. Compound **3** was assembled by segment coupling in solution as described [34]. Analytical HPLC was performed with a Rainin-Dynamax and Diode Array Detector (Woburn, MA), and preparative HPLC with a Rainin-Dynamax/SD1 and UV-Detector.

Ion channel activity

Planar lipid membranes were prepared by painting a solution of asolectine in *n*-decane (25 mg·mL^{-1}) over the aperture of a polystyrene cuvette with a diameter of 0.15 mm. All experiments were performed at ambient temperature. The cation solution at a concentration of 1 M was unbuffered. Compound **3**, dissolved in methanol, was added to one side of the

cuvette (final concentration in the cuvette 1 pM). Current detection and recording were performed with a patch-clamp amplifier Axopatch 200B, a Digidata A/D converter and pClamp6 software (Axon Instruments, Foster City, CA, USA). The acquisition frequency was 5 kHz. The data were filtered with a digital filter at 50 Hz for further analysis.

CD spectra

CD spectra were recorded with a Jasco-710 spectrometer. For the preparation of DMPC micelles, **3** and DMPC were dissolved in trifluoroethanol in a round-bottomed flask and sonicated at 50 °C for 30 min to obtain a homogeneous solution. The solvent was removed *in vacuo* to produce a thin film in the flask. Water was added and the mixture was sonicated at 50 °C for 30 min. The clear micellar solution thus prepared should be used on the same day for CD measurements.

NMR spectroscopy

3–Cs^+ complex in $CDCl_3/CD_3OH$ (1 : 1, v/v) at 3 mM was used for NMR experiments. DQF-COSY, TOCSY and NOESY experiments were performed on a Bruker Avance-800 spectrometer at 293 K. NMR titration and variable temperature ^{1}H-NMR spectra were recorded on a Bruker DRX-500 spectrometer. WATERGATE was used to suppress H_2O signal in 1D measurements. NOESY spectra were recorded with WATERGATE and at mixing times of 150 and 300 ms. DQF-COSY and TOCSY spectra were collected with a presaturation (3 s at 60 dB). 1D spectra were acquired with 65 536 data points, while 2D spectra were collected using 4096 points in t_2 and 512 t_1 increments. Typical experiment time for the 2D measurements was about 12 h.

NMR constraints

From $^3J_{\alpha N}$, 25 torsion angles ϕ were derived (not including glycine). Based on the volume integrals of the NOE cross-peaks of NOESY spectra at 150 ms, distance constraints were obtained: 1.8–2.4 Å for strong peaks, 1.8–3.5 Å for medium peaks, and 1.8–5.5 Å for weak peaks.

Structure calculation

Structure calculation was carried out by DYANA built in SYBYL 6.8, with the above constraints as input to the simulated annealing protocol and 50 random initial structures. Standard parameters of DYANA were applied. The temperature was raised to 9700 K (8.0 temperature units in DYANA) and then slowly cooled down to 0 K in 4000 steps. The resulting structures were further energy-minimized using Powell function in 1000 steps. The acceptable final structures had violations of target function of 0.3 $Å^2$, distance constraints of 0.2 Å, and torsion angle constraints of 5°. A final set of 11 structures with an average rmsd for the backbone of 0.45 Å was obtained.

Mass spectroscopy

Mass spectra were recorded with Applied Biosystems Q-Star under ESI-TOF conditions.

Acknowledgements

We acknowledge financial support from the Deutscher Akademischer Austausch Dienst (DAAD), Deutsche Forschungsgemeinschaft (DFG), Fonds der Chemischen Industrie and the VW-Stiftung. We thank Dr A. Knoll (Humboldt University) for assistance with single-channel current measurements, and D. Bockelmann for help with the 800-MHz NMR measurements.

References

1 Hille B (2001) *Ion Channels of Excitable Membranes*. Sinauer, Sunderland, MA.
2 Jiang Y, Lee A, Chen J, Cadene M, Chait BT & MacKinnon R (2002) Crystal structure and mechanism of a calcium-gated potassium channel. *Nature* **417**, 515–522.
3 Dutzler R, Campbell EB, Cadene M, Chait BT & MacKinnon R (2002) X-ray structure of a ClC chloride channel at 3.0 Å reveals the molecular basis of anion selectivity. *Nature* **415**, 287–294.
4 Kuo A, Gulbis JM, Antcliff JF, Rahman T, Lowe ED, Zimmer J, Cuthbertson J, Ashcroft FM, Ezaki T & Doyle DA (2003) Crystal structure of the potassium channel KirBac1.1 in the closed state. *Science* **300**, 1922–1926.
5 Koert U, Al-Momani L & Pfeifer JR (2004) Synthetic ion channels. *Synthesis* 1129–1146.
6 Gokel GW & Mukhopadyay A (2001) Synthetic models of cation-conducting channels. *Chem Soc Rev* **30**, 274–286.
7 Kobuke Y (1997) Artificial ion channels. *Adv Supramol Chem* **4**, 163–210.
8 Akerfeldt KS, Lear JD, Wasserman ZR, Chung LA & DeGrado WF (1993) Synthetic peptides as models for ion channel proteins. *Acc Chem Res* **26**, 191–197.
9 Eggers PK, Fyles TM, Mitchell KDD & Sutherland T (2003) Ion channels from linear and branched bola-amphiphiles. *J Org Chem* **68**, 1050–1058.
10 Yoshino N, Satake A & Kobuke Y (2001) An artificial ion channel formed by a macrocyclic resorcin. *Angew Chem Int Ed* **40**, 457–459.
11 Pregel MJ, Jullien L & Lehn J-M (1992) Towards artificial ion channels: transport of alkali metal ions across liposomal membranes by 'bouquet' molecules. *Angew Chem Int Ed Engl* **31**, 1637–1640.

12 Vescovi A, Knoll A & Koert U (2003) Synthesis and functional studies of THF-gramicidin hybrid ion channels. *Org Biomol Chem* **1**, 2983–2997.
13 Arndt H-D, Knoll. A & Koert U (2001) Cyclohexylether δ-amino acids: new leads for selectivity filters in ion channels. *Angew Chem Int Ed Engl* **40**, 2076–2078.
14 Voyer N & Robitaille M (1995) A novel artificial ion channel. *J Am Chem Soc* **117**, 6599–6600.
15 Sakai N & Matile S (2003) Synthetic multifunctional pores: lessons from rigid-rod β-barrels. *Chem Commun* **21**, 2514–2523.
16 Chadwick DJ & Cardew G (1999) *Gramicidin and Related Ion-Channel Forming Peptides*. Wiley, Chichester.
17 Koeppe RE & Andersen OS (1996) Engineering the gramicidin channel. *Annu Rev Biophys Biomol Struct* **25**, 231–258.
18 Borisenko V, Burns DC, Zhang Z & Woolley GA (2000) Optical switching of ion–dipole interactions in a gramicidin channel analoque. *J Am Chem Soc* **122**, 6364–6370.
19 Urry DW (1972) The gramicidin A transmembrane channel: a proposed π(L,D) helix. *Proc Natl Acad Sci USA* **68**, 672–676.
20 Arseniev AS, Barsukov AL, Bystrov IL, Lomize VF, Ovchinnikov AL & Yu A (1985) ^{1}H-NMR-study of gramicidin-A transmembrane ion channel. *FEBS Lett* **186**, 168–174.
21 Bystrov VF, Arseniev AS, Barsukov VL, Golovanov AP & Maslennikikov IV (1990) The structure of the transmembrane channel of gramicidin A: NMR study of its conformational stability and interaction with divalent cations. *Gazz Chim Ital* **120**, 485–491.
22 Ketchem RR, Hu W & Cross TA (1993) High resolution conformation of gramicidin A in a lipid-bilayer by solid state NMR. *Science* **261**, 1457–1460.
23 Bystrov VF & Arseniev AS (1988) Diversity of the gramicidin A spatial structure. Two-dimensional ^{1}H NMR study in solution. *Tetrahedron* **44**, 925–940.
24 Wallace BA (1998) Recent advances in the high resolution structures of bacterial channels: gramicidin A. *J Struct Biol* **121**, 123–141.
25 Allen TW, Andersen OS & Roux B (2004) Energetics of ion conduction through the gramicidin channel. *Proc Natl Acad Sci USA* **101**, 117–122.
26 Koeppe RE II, Sigworth FJ, Szabo G, Urry DW & Woolley A (1999) Gramicidin channel controversy: the structure in a lipid environment. *Nat Struct Biol* **6**, 609.
27 Cross TA, Arseniev A, Cornell BA, Davis JH, Killian JA, Koeppe RE II, Nicholson LK, Separovic F & Wallace BA (1999) Gramicidin channel controversy: revisited. *Nat Struct Biol* **6**, 610–611.
28 Burkhart BM & Duax WL (1999) Gramicidin channel controversy: reply. *Nat Struct Biol* **6**, 611–612.
29 Stankovic CJ, Heinemann SH, Delfino JM, Sigworth FJ & Schreiber SL (1989) Transmembrane channels based on tartaric acid–gramicidin A hybrids. *Science* **244**, 813–817.
30 Schrey A, Vescovi A, Knoll A, Rickert C & Koert U (2000) Synthesis and functional studies of a membrane-bound THF-gramicidin cation channel. *Angew Chem Int Ed Engl* **39**, 900–902.
31 Arndt H-D, Knoll A & Koert U (2001) Synthesis of minigramicidin ion channels and test of their hydrophobic match with the membrane. *Chembiochem* **3**, 221–223.
32 Arndt H-D, Bockelmann D, Knoll A, Lamberth S, Griesinger C & Koert U (2002) Cation control in functional helical programming: structures of a D,L-peptide ion channel. *Angew Chem Int Ed Engl* **41**, 4062–4065.
33 Chen Y, Tucker A & Wallace BA (1996) Solution structure of a parallel left-handed double helical gramicidin-A determined by 2D ^{1}H NMR. *J Mol Biol* **264**, 757–769.
34 Arndt H-D, Vescovi A, Schrey A, Pfeifer JR & Koert U (2002) Solution phase synthesis and purification of the minigramicidin ion channels and a succinyl-linked gramicidin. *Tetrahedron* **58**, 2789–2801.
35 Gratias R & Kessler H (1998) Molecular dynamics study on microheterogeneity and preferential solvation in methanol/chloroform mixtures. *J Phys Chem B* **102**, 2027–2031.
36 Wüthrich K (1986) *NMR of Proteins and Nucleic Acids*. Wiley, New York.
37 Güntert P, Mumenthaler C & Wüthrich K (1997) Torsion angle dynamics for NMR structure calculation with the new program DYANA. *J Mol Biol* **273**, 283–298.
38 Tassin-Moindrot S, Caille A, Douliez J-P, Marion D & Vovelle F (2000) The wide binding properties of a wheat nonspecific lipid transfer protein: solution structure of a complex with prostaglandin B_2. *Eur J Biochem* **267**, 1117–1124.
39 Güntert P, Braun W, Billeter M & Wüthrich K (1989) Automated stereospecific ^{1}H NMR assignments and their impact on the precision of protein structure determinations in solution. *J Am Chem Soc* **111**, 3997–4004.
40 Laskowski RA, Rullmann JAC, MacArthur MW, Kaptein R & Thornton JM (1996) AQUA and PROCHECK-NMR: programs for checking the quality of protein structures solved by NMR. *J Biomol NMR* **8**, 477–486.

Supplementary material

The following material is available from http://www.blackwellpublishing.com/products/journals/suppmat/EJB/EJB4531/EJB4531sm.htm

Fig. S1. DQF-COSY spectrum in the region of (F_2) 9.4–7.7 p.p.m. and (F_1) 6.0–3.4 p.p.m. (NH-αH finger-

print region) of **3** in $CDCl_3/CD_3OH$ (1 : 1, v/v) at 293 K.

Fig. S2. Selected ^{1}H-NMR spectra in the region of 11.0–7.9 p.p.m. (NH region) of the titration of **3** with CsCl in $CDCl_3/CD_3OH$ (1 : 1, v/v) at 293 K. The spectra were recorded on a Bruker DRX-500 spectrometer. The attached labels show the concentration of CsCl, where 10.9 mM was found to be the saturation point.

Table S1. Assignment table.

Table S2. Coupling constants ^3JNHαH (Hz) and the calculated torsion angles ϕ.